TÜBİTAK

**Turkish Journal of Medical Sciences**

**http://journals.tubitak.gov.tr/medical/**

**Research Article**

Turk J Med Sci
(2014) 44: 448-453
© TÜBİTAK
doi:10.3906/sag-1212-12

# Diastolic function of the right ventricle is impaired in experimental type 2 diabetic rat models

**Ya MIAO[1,*], Wei ZHANG[2], Yuan ZHONG[1], Ming ZHONG[2], Xiao MA[2]**

[1]Department of Geriatrics, Shanghai Jiaotong University Affiliated Sixth People's Hospital, Shanghai, P.R. China
[2]Department of Cardiology, Qilu Hospital Affiliated to Shandong University, Ji'nan, P.R. China

**Received:** 04.12.2012 • **Accepted:** 22.04.2013 • **Published Online:** 31.03.2014 • **Printed:** 30.04.2014

**Aim:** To evaluate diastolic function alterations of the right ventricle (RV) by echocardiography in type 2 diabetic rat models.

**Materials and methods:** Male Wistar rats were divided into 2 groups: a control group (n = 8) and a diabetic group (n = 16, with 11 remaining at the end of the experiment), which was fed a high-fat and high-calorie diet and injected with streptozotocin (STZ). RV diastolic functional alteration of rat models was studied by the tricuspid flow Doppler (Ep, Ap, and Ep/Ap) and tissue Doppler imaging (TDI) (Em, Am, and Em/Am) of the lateral tricuspid annulus. RV structural alteration of rat models was studied by standard 2D and M-mode echocardiography.

**Results:** Compared with the control group rats, at the 12th week after STZ injection, the rats of the diabetic group developed RV diastolic dysfunction, lower Em, and lower ratios (Ep/Ap, Em/Am). At the end of the experiment, at the 16th week after STZ injection, the rats of the diabetic group showed further decreased Ep, Em, and ratios (Ep/Ap, Em/Am) and significantly higher RV diameters compared with the control group rats.

**Conclusion:** We demonstrated that the diastolic dysfunction of the RV was the earliest complication observed in type 2 diabetic rat models, using TDI and tricuspid flow Doppler. TDI showed a high sensitivity in detecting changes of RV diastolic function.

**Key words:** Right ventricle, diastolic function, diabetic cardiomyopathy, echocardiography, rats

## 1. Introduction

Diabetes-induced myocardial diseases are the primary causes of morbidity and mortality in patients with diabetes mellitus (DM) (1). In 1972, Rubler et al. described a special type of diabetes-induced myocardial disease as the development of heart failure in diabetic subjects with the absence of ischemic, hypertension, and valvular heart disease, which was called diabetic cardiomyopathy (DCM) (2). The existence of DCM has been confirmed as evidence for the presence of myocardial dysfunction in diabetic patients without other heart diseases. Fang et al. reported that diabetic patients without overt heart disease demonstrate evidence of systolic dysfunction and increased myocardial reflectivity (3), which was in accordance with other studies in diabetic patients (4,5). The findings of myocardial impairment are similar in type 1 and type 2 diabetes mellitus (5,6). In animal experiments, Kim et al. described increased heart indexes and impaired mitral annulus velocity in diabetic rats (7).

As far as cardiac change of diabetic subjects is concerned, the left ventricle (LV) is generally paid more attention. Some recent findings indicated that myocardial damage in patients with diabetes affects diastolic dysfunction before systolic function, and it will be more significant for early diagnosis in order evaluate the outcomes of preclinical diastolic dysfunction in diabetic patients (8,9). Although it has been underestimated in the past, the contribution of the right ventricle (RV) function to overall myocardial contractility is considerable. However, relatively limited data exist for RV changes in the diabetic population, identified via noninvasive echocardiography, especially for RV diastolic function. The purpose of the present study is to assess RV structural and functional alteration, and especially RV diastolic function, by using echocardiography, including standard 2D, M-mode, conventional Doppler, and tissue Doppler imaging (TDI) echocardiography, in fat-fed, streptozotocin (STZ)-induced type 2 diabetic rat models.

* Correspondence: nning-my@163.com

## 2. Methods

### 2.1. Animal procedures

Male Wistar rats (weighing 180–220 g) were obtained from the Animal Center of the Shandong University (Jinan, China) and were randomly divided into the control group (n = 8) or the diabetic group (n = 16). Diabetic group rats were fed a high-fat and high-calorie diet (total 20 KJ/g and 25% fat), and after 5 weeks, they were injected with a single dose of STZ (30 mg/kg). Control group rats were fed a standard chow diet consisting of a total of 14 KJ/g and 8% fat. Details of the type 2 diabetic rat model process were published in our previous study (10).

Fasting blood glucose (FBG) was measured by glucose oxidase method in an automatic biochemical analyzer (DVI 1650), and fasting insulin (FINS) was measured with a radioimmunoassay (RIA) kit (BNIBT Co, China) in a RIA counter (XH-6010). The standard for diabetic rats was FBG ≥ 11.1 mmol/L in 2 consecutive analyses, and the insulin sensitivity index [ISI = ln (FBG × FINS)$^{-1}$] was lower than that of the control group. Rats were subsequently maintained for 16 weeks. The study conformed to the Guide for the Care and Use of Laboratory Animals published by the US National Institutes of Health.

### 2.2. Echocardiography

Rats were anesthetized with chloral hydrate (30 mg/kg). Their chests were shaved, and echocardiography was performed on each rat at baseline, at the 12th week after STZ or buffer injection, and at the end of the experiment (16th week after STZ or buffer injection) using a standard commercial ultrasound machine (HP SONOS 7500; Hewlett-Packard, USA) with a 5–12 MHz transducer. Meanwhile, the 3-lead electrocardiogram was recorded from the front limbs and the right hind limb. Standard 2D, 2D-guided M-mode, pulsed-wave Doppler, and TDI echocardiography were performed on all rats by a single experienced operator blinded to different groups. All images were saved in magneto optical disks for offline analysis. All of the parameters were averaged by at least 3 consecutive cardiac cycles.

### 2.3. Standard 2D and M-mode echocardiographic measurements

Standard 2D images of each rat were obtained via the parasternal long and short axis views and the apical 4-chamber view, and 2D-guided M-mode images were obtained via the parasternal long axis view. The right cardiac end-diastolic diameters, including RV diameter (RVD), right atrium left-to-right diameter (RADlr), and right atrium anterior-to-posterior diameter (RADap), were measured from the standard 2D images. The end-diastolic wall thickness, including interventricular septum (IVS) and RV free wall thickness (RVFW), were obtained by M-mode.

### 2.4. Conventional Doppler measurements

The same ultrasound machine was used to acquire the pulsed-wave Doppler spectra of the tricuspid inflow. The sample volume was placed between the tips of tricuspid leaflets in the apical 4-chamber view. The Doppler beam was aligned parallel to flow direction to obtain the maximum velocity, which was identified on a color Doppler image. The peak early transtricuspid filling velocity (Ep), peak transtricuspid atrial filling velocity during late diastole (Ap), and their ratio (Ep/Ap) were measured to evaluate the right ventricular function. Measurements were averaged from 3 end-expiratory cycles.

### 2.5. Tissue Doppler measurements

Lateral tricuspid annular tissue Doppler velocities were recorded by pulsed-wave TDI in the apical 4-chamber views. Using the same probe with low filter and gain settings, the smallest sample volume was placed at the lateral corner of the tricuspid annulus. Signals were obtained from 3 end-expiratory cycles, and averages were made for the systolic and diastolic velocities. Pulse-wave TDI results of the tricuspid annulus were characterized by 1 myocardial systolic wave (systolic maximal velocity, Sm) and 2 diastolic waves, early-diastolic maximal velocity (Em) and atrial-contraction maximal velocity (Am), and their ratio (Em/Am).

### 2.6. Statistical Analysis

SPSS 18.0 was used in our study. All values are expressed as mean ± SD. Unpaired Student's t-tests were used to compare variable differences between the 2 groups. Results were considered statistically significant if $P < 0.05$.

## 3. Results

### 3.1. The differences of FBG and ISI in control group and diabetic group

In the diabetic group, 3 rats died from ketosis, infection, or other diabetic complications and 2 rats failed to meet the diagnostic criteria of diabetes. There were 11 rats in the diabetic group and 8 rats in the control group at the end of the experiment.

There were no significant differences in FBG and ISI between the 2 groups (Figures 1a and 1b). Diabetic group rats, which were fed a 4-week high-calorie diet, showed low ISI compared to the control group rats, which showed a higher insulin resistance. The difference of ISI between the 2 groups remained until the end of the experiment. As expected, the diabetic group rats had higher levels of FBG than the control group rats from the fifth week after STZ injection until the end of the experiment.

### 3.2. RV structural changes in the control group and the diabetic group

RV structural changes were measured by standard 2D and M-mode echocardiography and are summarized in Table 1. At the 12th week after STZ or buffer injection, there was

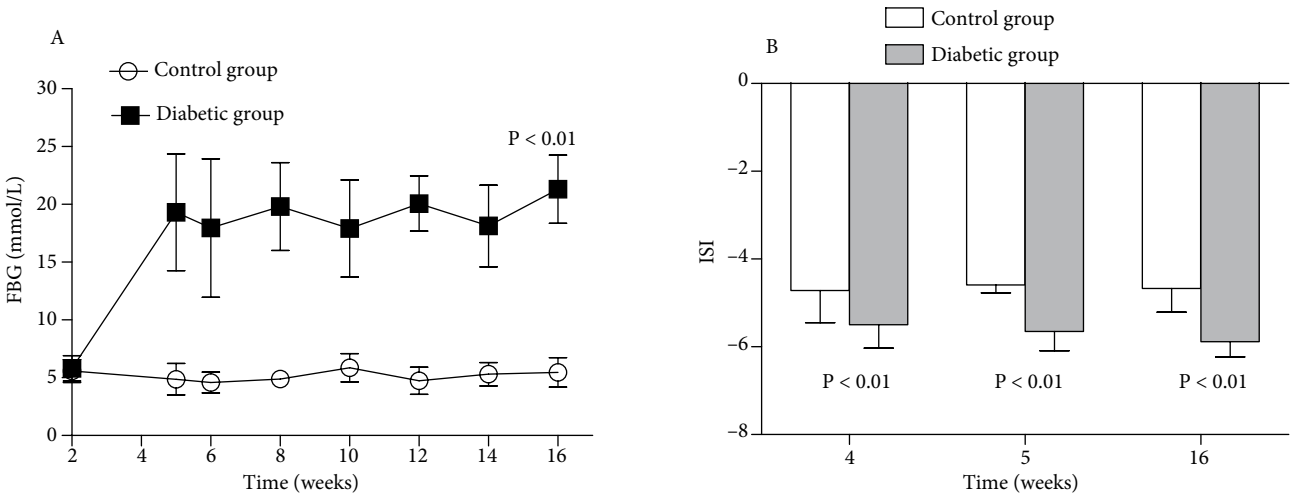


**Figure 1.** FBG (a) and ISI (b) in the control group and the diabetic group. FBG = Fasting blood glucose; ISI = insulin sensitivity index; n = 8 for control group; n = 11 for diabetic group.

**Table 1.** RV structural changes in the control group and the diabetic group. STZ = streptozotocin; RADap = right atrium anterior-to-posterior diameter; RADlr = right atrium left-to-right diameter; RVD = right ventricular diameters; IVS = interventricular septum; RVFW = right ventricular free wall thickness; n = 8 for control group; n = 11 for diabetic group.

| | | RADap (mm) | RADlr (mm) | RVD (mm) | IVS (mm) | RVFW (mm) |
|---|---|---|---|---|---|---|
| At the 12th week | Control group | 4.39 ± 1.12 | 4.58 ± 1.23 | 2.90 ± 0.43 | 1.69 ± 0.24 | 0.61 ± 0.11 |
| | Diabetic group | 4.56 ± 1.19 | 4.85 ± 1.02 | 3.02 ± 0.66 | 1.75 ± 0.29 | 0.63 ± 0.17 |
| At the end of the experiment | Control group | 4.42 ± 1.17 | 4.61 ± 1.40 | 2.97 ± 0.19 | 1.74 ± 0.16 | 0.63 ± 0.10 |
| | Diabetic group | 4.66 ± 1.09 | 5.07 ± 0.41 | 3.25 ± 0.25* | 1.84 ± 0.19 | 0.66 ± 0.12 |

no significant difference in any structural indices of RV in the 2 groups. At the end of the experiment, although the measurements of RADap, RADlr, IVS, and RVFW were greater in the diabetic group than in the control group, these findings did not reach statistical significance. However, by comparison with the control group, the diabetic group showed significantly higher RVD ($P < 0.05$).

### 3.3. RV diastolic function in the control group and the diabetic group

The RV diastolic function was evaluated by conventional flow Doppler (Figure 2a) and TDI (Figure 2b). The results of the 2 groups are shown in Table 2, which includes the diastolic function parameters Ep, Em, and their ratios (Ep/Ap, Em/Am), and systolic function parameters (Sm). At the 12th week after the STZ or buffer injection, the Ep/Ap of the tricuspid flow Doppler in the diabetic group and the Em and Em/Am of TDI were lower than those of the control group. At the end of the experiment, according to the flow Doppler, the tricuspid Ep was significantly lower in the diabetic group, with consequently significantly lower Ep/Ap. The TDI of tricuspid annulus showed that Em and Em/Am in the diabetic group were lower than those in the control group. Sm and Am in the 2 groups were similar. It can be concluded that the RV diastolic dysfunction was visible in the type 2 diabetic rats.

## 4. Discussion

To understand diabetic cardiac dysfunction, we developed a rat model of type 2 diabetes. Type 2 diabetes is characterized by reduced insulin sensitivity (insulin resistance) and higher blood glucose. In the present experiment, insulin resistance was induced by a high-fat diet initially (11). Thereafter, a low-dose STZ injection slightly reduced the number of β cells, which eventually resulted in hyperglycemia (12). The rat strain well resembled the natural history and metabolic characteristics of human type 2 diabetes.

The detection of subclinical cardiac dysfunction in diabetic patients may provide an approach for identifying high-risk individuals who may benefit from earlier and more active intervention to prevent heart failure. Subclinical cardiac dysfunction is common in patients

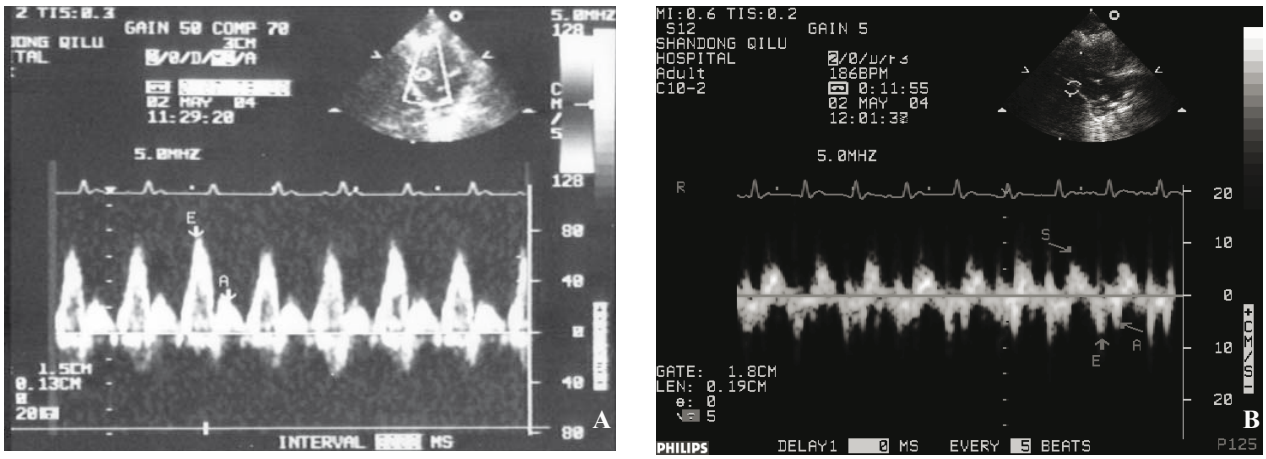


**Figure 2.** Tricuspid inflow Doppler (a) and TDI (b) of tricuspid annulus in rats.

**Table 2.** RV diastolic function in the control group and the diabetic group. STZ = streptozotocin; TDI = tissue Doppler imaging; Ep = the peak early transtricuspid filling velocity; Ap = peak transtricuspid atrial filling velocity during late diastole; Ep/Ap = the ratio of Ep and Ap; Em = early-diastolic maximal velocity; Am = atrial-contraction maximal velocity; Em/Am = the ratio of Em and Am; Sm = systolic maximal velocity; n = 8 for control group; n = 11 for diabetic group; * = P < 0.05; ** = P < 0.01.

| | | Tricuspid inflow Doppler | | | TDI | | | |
|---|---|---|---|---|---|---|---|---|
| | | Ep (cm/s) | Ap (cm/s) | Ep/Ap | Em (cm/s) | Am (cm/s) | Em/Am | Sm (cm/s) |
| At the 12th week | Control group | 81.61 ± 18.12 | 38.40 ± 7.88 | 2.14 ± 0.29 | 6.42 ± 1.18 | 4.30 ± 0.80 | 1.51 ± 0.24 | 5.61 ± 1.01 |
| | Diabetic group | 72.06 ± 14.01 | 42.38 ± 5.81 | 1.71 ± 0.34* | 4.51 ± 1.30* | 4.82 ± 0.25 | 0.94 ± 0.29** | 5.04 ± 1.18 |
| At the end of the experiment | Control group | 84.11 ± 12.12 | 39.15 ± 6.09 | 2.21 ± 0.56 | 6.30 ± 0.93 | 4.37 ± 0.92 | 1.49 ± 0.34 | 5.83 ± 1.28 |
| | Diabetic group | 70.25 ± 12.79** | 43.37 ± 6.07 | 1.58 ± 0.38** | 4.17 ± 1.28** | 5.41 ± 1.25 | 0.81 ± 0.33** | 4.81 ± 1.34 |

with diabetes, and in these studies, some reported that cardiac diastolic dysfunction represents an early stage of myocardial damage in patients with diabetes, without any clinical manifestations (8,9). Although RV dysfunction has not been paid due attention in the past, in recent years, researchers have gradually realized that RV dysfunction is relevant and is an independent predictor in a variety of disease states (13,14). Van den Brom reported RV systolic dysfunction in Zucker diabetic fatty rats (15). Several clinical studies using echocardiography have also shown RV dysfunction in patients with diabetes (16,17). However, in the above studies, the alteration of RV diastolic function, which should be paid more attention, was not studied. In the present study, we detected the changes of RV function, especially RV diastolic function, in type 2 diabetic rats using pulsed wave Doppler and TDI.

During the early stages of cardiac metabolic impairments, the heart goes through a phase of adjustment to the newly appearing metabolic disorders, and the normal myocardial structure and architecture, such as the wall thickness and the internal dimensions of cardiac cavities, are maintained. However, lesions occurring at a myocytic level are functionally expressed and can be detected with modern echocardiographic techniques. At the 12th week after STZ injection, this study showed that the tricuspid Ep/Ap ratio decreased in diabetic rats. The TDI of tricuspid annulus showed that Em and Em/Am in the diabetic group were lower than those in the control group. However, there were no significant differences of RV wall thickness and internal dimensions in the 2 groups at the 12th week after the STZ injection. Karamitsos et al. described a similar finding by demonstrating RV dysfunction prior to the structural abnormality in type 1 diabetic patients (18). However, as the experiment continued, the changes in the structure of the myocardium became visible. At the end of the current experiment, at the 16th week after STZ injection, diabetic rats showed significantly higher RVD compared to control rats. However, the other measurements of the right cardiac structure still failed to reach statistical significance.

As we mentioned above, at the 12th week after STZ injection, RV diastolic dysfunction could be found by echocardiography. At the 16th week after STZ injection, the diabetic rats showed more deteriorated RV functions, characterized by decreased Ep, Em, and their ratios (Ep/Ap, Em/Am), which reflected impaired diastolic function of the RV. TDI can confirm the presence of diastolic dysfunctions, as well as systolic dysfunction: Em and Em/Am are for RV diastolic function and Sm is for the RV systolic function. In our study, we did not find evidence of any significant difference in Sm between the 2 groups throughout the whole experiment. This result was in accordance with the report by Karamitsos et al. (18).

Furthermore, in the present study, TDI of tricuspid annulus showed higher sensitivity in detection of RV diastolic function than the conventional flow Doppler of tricuspid annulus. As far as TDI was concerned, in addition to the ratio of Em/Am, Em showed visible differences between the 2 groups at both the 12th week after STZ injection and the 16th week after STZ injection. However, at the 12th week after STZ injection, only the Ep/Ap ratio of the 2 groups reached statistical significance, and Ep of the 2 groups failed to reach statistical significance in the conventional flow Doppler of tricuspid annulus. Boyer et al. confirmed that TDI has a rate of sensitivity of up to 63% against the 50% of the pulsed Doppler (19).

Collectively, our type 2 diabetic rat model was a good choice for studying diabetic myocardial disease. Moreover, this study demonstrated that diastolic dysfunction of RV was the earliest complication observed in DCM. The systolic dysfunction of RV was not evident in our study. As a modern echocardiographic technique, TDI showed high sensitivity in detecting changes of RV function. Diabetes is associated with profound changes in cardiac metabolism, structure, and function. The development of diabetic myocardial disease is multifactorial. The main pathophysiological mechanisms that are implicated are possibly as follows: the deficiency of energy utilization in myocardial cells, hypertrophy and fibrosis, microvascular remodeling, homeostatic disorders of calcium, the abnormal activation of the neurohormonal axis, the overexpression of the inflammatory process, and oxidative stress (20–23).

Further studies about the pathological evaluation of RV in diabetic subjects are necessary. We will follow up with another study to look for the RV pathological changes and the probable mechanism causing RV impairment in diabetic patients. We also plan to evaluate the development of RV function in patients with type 2 diabetes mellitus, which will be more helpful for clinical patients. There is a shortcoming in our study that may limit the interpretation of the results. No RV systolic dysfunction was found in our study. Apart from simply observing no obvious systolic dysfunction, another possible reason for this result was the lack of appropriate indexes for RV systolic function. Other indexes for RV systolic function, such as tricuspid annular plane systolic excursion, will be included in our future studies.

**Acknowledgment**

This study was supported by the National Nature Science Foundation (81300933) and the Shanghai Jiaotong University Interdisciplinary Study Foundation of Medicine and Engineering (YG2011MS46).

**References**

1. Mytas DZ, Stougiannos PN, Zairis MN, Foussas SG, Pyrgakis VN, Kyriazis IA. Diabetic myocardial disease: pathophysiology, early diagnosis and therapeutic options. J Diabetes Complications 2009; 23: 273–82.
2. Rubler S, Dlugash J, Yuceoglu YZ, Kumral T, Branwood AW, Grishman A. New type of cardiomyopathy associated with diabetic glomerulosclerosis. Am J Cardiol 1972; 30: 595–602.
3. Fang ZY, Yuda S, Anderson V, Short L, Case C, Marwick TH. Echocardiographic detection of early diabetic myocardial disease. J Am Coll Cardiol 2003; 41: 611–7.
4. Poantă L, Fodor D, Albu A. Left ventricular function in patients with uncomplicated well-controlled diabetes mellitus. Med Ultrason 2010; 12: 184–7.
5. Ernande L, Rietzschel ER, Bergerot C, De Buyzere ML, Schnell F, Groisne L, Ovize M, Croisille P, Moulin P, Gillebert TC et al. Impaired myocardial radial function in asymptomatic patients with type 2 diabetes mellitus: a speckle-tracking imaging study. J Am Soc Echocardiogr 2010; 23: 1266–72.
6. Chillo P, Rieck AE, Lwakatare J, Lutale J, Gerdts E. Left atrial volume index as a marker of left ventricular diastolic dysfunction in asymptomatic Tanzanian diabetic patients. Blood Press 2013; 22: 86–93.
7. Kim DH, Kim YJ, Kim HK, Chang SA, Kim MS, Sohn DW, Oh BH, Park YB. Usefulness of mitral annulus velocity for the early detection of left ventricular dysfunction in a rat model of diabetic cardiomyopathy. J Cardiovasc Ultrasound 2010; 18: 6–11.
8. Patil MB, Burji NP. Echocardiographic evaluation of diastolic dysfunction in asymptomatic type 2 diabetes mellitus. J Assoc Physicians India 2012; 60: 23–6.
9. From AM, Scott CG, Chen HH. The development of heart failure in patients with diabetes mellitus and pre-clinical diastolic dysfunction a population-based study. J Am Coll Cardiol 2010; 55: 300–5.
10. Sun H, Zhong M, Miao Y, Ma X, Gong HP, Tan HW, Zhang Y, Zhang W. Impaired elastic properties of the aorta in fat-fed, streptozotocin-treated rats. Vascular remodeling in diabetic arteries. Cardiology 2009; 114: 107–13.

11. Zhang F, Ye C, Li G, Ding W, Zhou W, Zhu H, Chen G, Luo T, Guang M, Liu Y et al. The rat model of type 2 diabetic mellitus and its glycometabolism characters. Exp Anim 2003; 52: 401–7.
12. Pari L, Sankaranarayanan C. Beneficial effects of thymoquinone on hepatic key enzymes in streptozotocin-nicotinamide induced diabetic rats. Life Sci 2009; 85: 830–4.
13. Widya RL, van der Meer RW, Smit JW, Rijzewijk LJ, Diamant M, Bax JJ, de Roos A, Lamb HJ. Right ventricular involvement in diabetic cardiomyopathy. Diabetes Care 2013; 36: 457–62.
14. Karas MG, Kizer JR. Echocardiographic assessment of the right ventricle and associated hemodynamics. Prog Cardiovasc Dis 2012; 55: 144–60.
15. van den Brom CE, Bosmans JW, Vlasblom R, Handoko LM, Huisman MC, Lubberink M, Molthoff CF, Lammertsma AA, Ouwens MD, Diamant M et al. Diabetic cardiomyopathy in Zucker diabetic fatty rats: the forgotten right ventricle. Cardiovasc Diabetol 2010; 9: 25–31.
16. Vittos O, Toana B, Vittos A. Biomarkers and their involvement in the early diagnosis of right ventricular dysfunction in type 2 diabetes mellitus. J Med Life 2012; 5: 74–8.
17. Ng AC, Delgado V, Bertini M, van der Meer RW, Rijzewijk LJ, Hooi Ewe S, Siebelink HM, Smit JW, Diamant M, Romijn JA et al. Myocardial steatosis and biventricular strain and strain rate imaging in patients with type 2 diabetes mellitus. Circulation 2010; 122: 2538–44.
18. Karamitsos TD, Karvounis HI, Dalamanga EG, Papadopoulos CE, Didangellos TP, Karamitsos DT, Parharidis GE, Louridas GE. Early diastolic impairment of diabetic heart: the significance of right ventricle. Int J Cardiol 2007; 114: 218–23.
19. Boyer JK, Thanigaraj S, Schechtman KB, Pérez JE. Prevalence of ventricular diastolic dysfunction in asymptomatic, normotensive patients with diabetes mellitus. Am J Cardiol 2004; 93: 870–5.
20. Khullar M, Al-Shudiefat AA, Ludke A, Binepal G, Singal PK. Oxidative stress: a key contributor to diabetic cardiomyopathy. Can J Physiol Pharmacol 2010; 88: 233–40.
21. Selvaraju V, Joshi M, Suresh S, Sanchez JA, Maulik N, Maulik G. Diabetes, oxidative stress, molecular mechanism, and cardiovascular disease–an overview. Toxicol Mech Methods 2012; 22: 330–5.
22. Dobrin JS, Lebeche D. Diabetic cardiomyopathy: signaling defects and therapeutic approaches. Expert Rev Cardiovasc Ther 2010; 8: 373–91.
23. Liu JW, Liu D, Cui KZ, Xu Y, Li YB, Sun YM, Su Y. Recent advances in understanding the biochemical and molecular mechanism of diabetic cardiomyopathy. Biochem Biophys Res Commun 2012; 427: 441–3.